Check for updates

JOURNAL OF THE AMERICAN WATER RESOURCES ASSOCIATION

AMERICAN WATER RESOURCES ASSOCIATION

# A High-Resolution Land Data Assimilation System Optimized for the Western United States

*Jessica M. Erlingis, Matthew Rodell, Christa D. Peters-Lidard, Bailing Li, Sujay V. Kumar, James S. Famiglietti, Stephanie L. Granger, John V. Hurley, Pang-Wei Liu, and David M. Mocko*

**Research Impact Statement**: A publicly available 1-km land data assimilation system providing daily data from 1979–present has been developed to support water resources applications in the western United States.

ABSTRACT: The Western Land Data Assimilation System (WLDAS) is a custom instance of the NASA Land Information System that combines land surface parameters, meteorological forcing data, and satellite products within a land surface model to produce daily estimates of the water and energy budget variables for the western United States. WLDAS was configured through discussions with partners, with the goal of groundwater sustainability planning for the state of California in mind. The publicly available output dataset has a 1-km grid resolution and spans 1979–present, which makes it suitable for water resources assessments. The data are also able to contextualize the recent drought events in California. Assimilation of Leaf Area Index, which is demonstrated herein to improve simulation over agricultural areas in California, specifically in terms of evapotranspiration in irrigation regions, will be included along with other data assimilation in subsequent releases of WLDAS.

(KEYWORDS: land surface modeling; data assimilation; complex terrain; reanalysis.)

## INTRODUCTION

Much of the western United States (U.S.) exists in a near-constant state of freshwater scarcity, exacerbated by intermittent droughts. Annual assessments of alpine snowpack determine water resources allocations and decisions, and dependence on groundwater continues to increase to address the deficits from inadequate rainfall and surface water supplies (Faunt 2009; Famiglietti et al. 2011). The unsustainable use of groundwater may result in reduced groundwater storage, seawater intrusion, land subsidence, degraded water quality, and depletion of interconnected surface water (Wada et al. 2010; Gleeson et al. 2012; Famiglietti 2014; Liu et al. 2019). Reduced recharge to aquifers due to changes in precipitation and increases in evapotranspiration (ET), alongside increasing withdrawals, are likely to intensify these problems as the climate changes (Kundzewicz and Döll 2009; Taylor et al. 2013; Meixner et al. 2016; Niraula et al. 2017). In particular, California's population and economy are highly dependent on groundwater resources. More than 250 different crops, worth more than $17 billion USD per year, are grown in the Central Valley of California (Faunt 2009), and, in times of drought, pumping of groundwater for irrigation helps buffer agricultural impacts (Giordano 2009; Scanlon et al. 2012; Medellín-Azuara et al. 2015) but can result in the overdraft of resources.

The recent California drought of 2011–2017 was historic and costly. The calendar year of 2013 is the driest

Paper No. JAWR-20-0082-P of the *Journal of the American Water Resources Association* (JAWR). Received June 30, 2020; accepted February 2, 2021. © 2021 American Water Resources Association. **Discussions are open until six months from issue publication**.

Earth System Science Interdisciplinary Center (Erlingis, Li), University of Maryland College Park, Maryland, USA; NASA Goddard Space Flight Center (Rodell; Peters-Lidard; Kumar), Greenbelt, Maryland, USA; Global Institute for Water Security (Famiglietti), University of Saskatchewan Saskatoon, Saskatchewan, Canada; Jet Propulsion Laboratory (Granger), California Institute of Technology Pasadena, California, USA; California State Water Resources Control Board (Hurley), Sacramento, California, USA; Science Systems and Applications, Inc. (Liu), Lanham, Maryland, USA; and Science Applications International Corporation (Mocko), Beltsville, Maryland, USA (Correspondence to Erlingis: jessica.erlingislamers@nasa.gov).

*Citation*: Erlingis, J.M., M. Rodell, C.D. Peters-Lidard, B. Li, S.V. Kumar, J.S. Famiglietti, S.L. Granger, J.V. Hurley, P.-W. Liu, and D.M. Mocko. 2021. "A High-Resolution Land Data Assimilation System Optimized for the Western United States." *Journal of the American Water Resources Association* 1–19. https://doi.org/10.1111/1752-1688.12910.

in California in the instrumental record (1895–2020; Herring et al. 2014), and 2015 is the 14th driest (National Centers for Environmental Information 2020). Snowpack was reduced to 25% of the annual average in 2014 and 5% of the annual average in 2015 (Funk et al. 2014; Swain 2015). In order to avoid the negative outcomes caused by overdrafting aquifers in such crises, the state of California passed the Sustainable Groundwater Management Act in 2014 (https://water.ca.gov/Programs/Groundwater-Management/SGMA-Groundwater-Management), which led to the local establishment of more than 260 Groundwater Sustainability Agencies (GSAs) to manage groundwater resources.

A long-term, detailed estimate of the natural water budget and its variability in space and time for the entire state is useful to develop informed planning decisions required of the GSAs under the new law. An ideal system would be driven by consistent, high-quality meteorological input over a long record and have a sufficiently fine spatial resolution to capture the complex hydrological processes and spatial heterogeneity in mountainous regions. Numerical modeling of the land surface is a way to provide physically consistent, spatially and temporally continuous information about the water and energy budgets of the surface, subsurface, vegetation canopy, and snowpack. This is advantageous because *in situ* measurements of soil moisture, snow depth, and other relevant variables may be sparse and representative only of the conditions at a given point or of a limited domain. Remote sensing techniques offer more continuous observations of these variables that circumvent the need for interpolation (Famiglietti et al. 2015). Land data assimilation systems (LDASs) can help to bridge these gaps in hydrological information by optimally combining observations with knowledge of physical processes, as represented in the models (e.g., Rodell et al. 2004; Wang et al. 2009; Mo et al. 2012).

This paper describes the development of the Western Land Data Assimilation System (WLDAS) over the western U.S. and a collaborative effort between NASA scientists and the California State Water Resources Control Board (SWRCB). The software used for this project is described in the subsequent section followed by the model configuration. Demonstrations of the model capabilities are shown along with an evaluation of future enhancements to the current configuration.

## METHODS: OVERVIEW OF WLDAS

### *Land Information System*

The Land Information System (LIS; Kumar et al. 2006; Peters-Lidard et al. 2007) software developed at NASA Goddard Space Flight Center (GSFC) enables land surface parameter processing and simulation and multivariate data assimilation using multiple land surface models (LSM), within a single open-source framework (https://github.com/NASA-LIS/LISF). LIS includes preprocessing tools in the Land Data Toolkit (LDT; Arsenault et al. 2018); ensemble land surface modeling, data assimilation, and inverse modeling capabilities (Kumar et al. 2008; Harrison et al. 2012; Kumar et al. 2017); and postprocessing and analysis capabilities in the Land Verification Toolkit (LVT; Kumar et al. 2012). For WLDAS, the Noah-Multiparameterization (MP) version 3.6 LSM was used. The Noah-MP LSM (Niu et al. 2011; Yang et al. 2011) is an extension of the Noah LSM (Ek et al. 2003) and includes options for additional physical processes such as dynamic vegetation (based on Dickinson et al. 1998) and groundwater recharge, storage, and discharge with the Simple Groundwater Model (SIMGM; Niu et al. 2007). Noah-MP also simulates snowpack in multiple layers, which has been shown to improve simulations of snow water equivalent (SWE) compared with single-layer snowpack representations (Ma et al. 2017).

WLDAS is a custom instance of LIS and leverages previous LDAS development efforts including the Global Land Data Assimilation System (GLDAS; Rodell et al. 2004), the North American Land Data Assimilation System (NLDAS; Mitchell et al. 2004; Xia et al. 2012), the Famine Early Warning Systems Network Land Data Assimilation System (McNally et al. 2017), the U.S. Air Force 557th Weather Wing LDAS, and the National Climate Assessment Land Data Assimilation System (Jasinski et al. 2019; Kumar, Jasinski, et al. 2019).

### *Model Configuration*

The WLDAS domain and static land surface data are summarized in Table 1. The configuration options for the Noah-MP LSM are listed in Table 2. The model is run with a 15-min internal integration timestep on a $0.01° \times 0.01°$ grid over the area west of the Mississippi River (Figure 1; 25.06–52.93°N; 124.93–89.03°W); this finer grid represents an order of magnitude increase in spatial resolution over the currently operational NLDAS. The scale of WLDAS addresses the need for higher resolution land surface modeling and contributes toward the challenges outlined by Wood et al. (2011). WLDAS produces daily average output of variables ending at 0000 UTC. In WLDAS, a 2-m soil column is divided into four layers: 0–10 cm, 10–40 cm, 40–100 cm, and 100–200 cm below the surface. A dynamic vegetation model (Dickinson et al. 1998; Niu et al. 2011), which simulates carbon stores in the stem, roots, and leaves, was

TABLE 1. Model static parameters.

| Property | Description/dataset |
|---|---|
| Domain | 25.06–52.93°N 124.93–89.03°W |
| Time period | 1979–present |
| Temporal resolution | Daily–averaged |
| Soil layers | 0–10 cm, 10–40 cm, 40–100 cm, 100–200 cm |
| Grid spacing | 0.01° × 0.01° |
| Land cover | MODIS |
| Soil texture | STATSGO-FAO (1 km) |
| Greenness fraction | MODIS/NOAA-NCEP |
| Elevation | SRTM |
| Albedo | MODIS/NOAA-NCEP |

enabled. To ensure that the land surface was at an equilibrium state, the model was run once with NLDAS-2 forcing for the period 1979–2017 (spin-up) and restarted for the same period from a climatological restart file of the average of all December 31s. This approach minimizes the impact of a wet or dry year on initial conditions when the model is repeatedly run using forcing data from that single year (Rodell et al. 2005).

A diagram of the WLDAS product generation process is shown in Figure 2. The static land surface parameters such as land cover type, soil texture, and topography are first processed by LDT. Then meteorological forcing is downscaled by LIS, and the LSM is integrated forward in time to produce the output variables. If enabled, the data assimilation algorithm updates the model states based on remotely sensed observations during the LSM integration to produce the land surface water and energy budgets.

A key component of WLDAS development has been feedback and discussion with the SWRCB, facilitated by the NASA Western Water Applications Office (WWAO; https://wwao.jpl.nasa.gov/). WWAO has conducted needs assessments in major basins throughout the western U.S. and connected regional partners with NASA scientists and capabilities. In such assessments and subsequent project development meetings, the SWRCB has highlighted the need for high-resolution products, specifically satellite imagery, ET, precipitation, runoff, and groundwater recharge, in their domain. The WLDAS products can be used as additional data sources themselves or integrated into pre-existing hydrological modeling capabilities at SWRCB and at the GSAs. The use of LDASs, meteorological data, and satellite data that have been vetted and accepted by the scientific community is also advantageous.

TABLE 2. Model configuration options.

| Model process | Parameterization used |
|---|---|
| Vegetation | Dynamic vegetation |
| Stomatal resistance | Ball-Berry (Ball et al. 1987) |
| Runoff and groundwater | SIMGM (Niu et al. 2007) |
| Radiation transfer | Modified two-stream scheme (Niu and Yang 2004) |
| Snow surface albedo | CLASS (Verseghy 1991) |
| Precipitation phase (rain/snow) partitioning | Jordan (1991) |
| Surface layer drag coefficient | Monin-Obukhov |
| Supercooled liquid water | Niu and Yang (2006) |
| Frozen soil permeability | Niu and Yang (2006) |
| Lower boundary soil temperature | Noah |
| Snow and soil temperature time scheme | Semi-implicit |

Note: SIMGM, Simple Groundwater Model.

*Forcing Data*

LIS is run uncoupled from the atmosphere, that is, without two-way feedback to the atmosphere enabled, to reduce bias in the water and energy budgets at the surface. Noah-MP requires near-surface air temperature and specific humidity, incoming shortwave and longwave radiation, surface pressure, precipitation, and the 10-m $u$- and $v$- wind components as the meteorological forcing inputs. In this study, the NLDAS-2 forcing dataset (Xia et al. 2012) is used, which is largely derived from the 32-km North American Regional Reanalysis products (NARR; Mesinger et al. 2006). The NLDAS-2 forcing dataset is available at hourly timesteps and 0.125° grid spacing. The precipitation in the NLDAS dataset (Cosgrove et al. 2003) is derived from daily CPC gauge data (Higgins et al. 2000; Chen et al. 2008) and is temporally disaggregated to hourly temporal resolution using a hierarchy of Stage II radar precipitation data (Baldwin and Mitchell 1997), CMORPH data (Joyce et al. 2004), and 3-hourly NARR precipitation. Shortwave radiation fields from NARR are bias corrected using a monthly averaged diurnal cycle climatology derived from the Geostationary Operational Environmental Satellite using the University of Maryland Surface Radiation Budget Dataset (Pinker et al. 2003). Other fields are interpolated to the NLDAS-2 grid and adjusted for differences in topography between the NARR and NLDAS-2 datasets (Cosgrove et al. 2003).

In order to address the need for forcing data at even finer spatial scales over the complex topography that exists across the western U.S., the NLDAS-2 forcing data were downscaled to the 0.01° WLDAS model grid. Precipitation fields were spatially downscaled using the 800-m Parameter-Elevation Regressions on Independent Slopes Model (PRISM) monthly climatology of precipitation (Daly et al. 2008) to match the precipitation patterns over mountainous regions. The radiation fields were downscaled using a slope and aspect correction, which splits the incoming

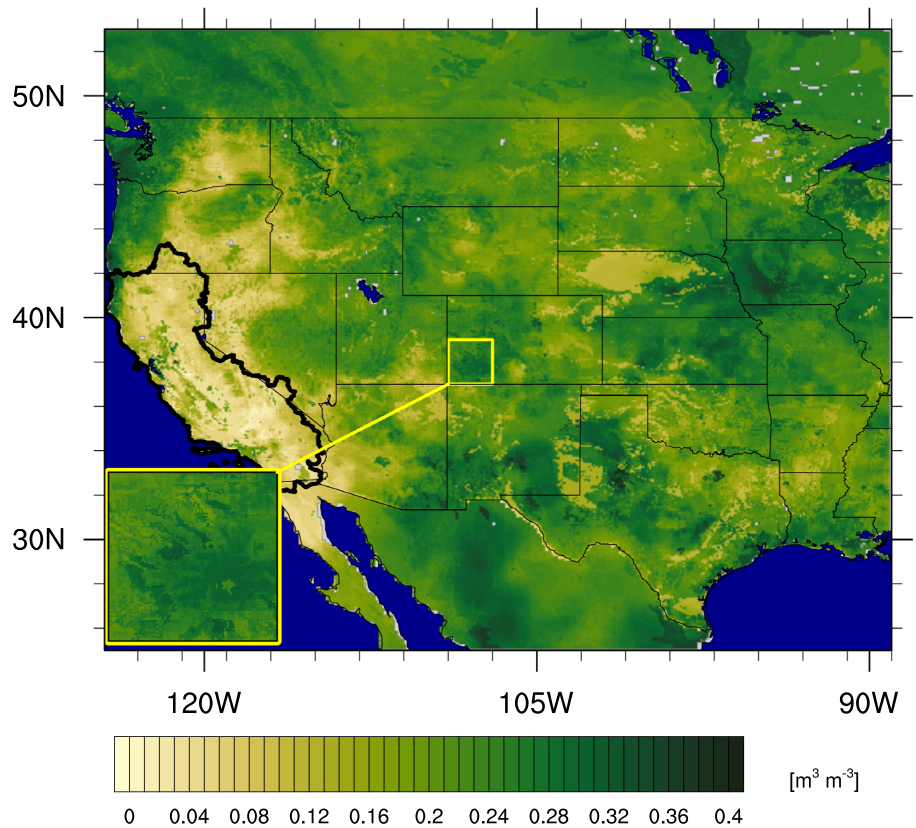


FIGURE 1. Simulated daily surface (0–10 cm) soil moisture at 00 UTC on 25 September 2014 over the Western Land Data Assimilation System (WLDAS) domain. The inset map highlights the 1-km grid spacing of WLDAS products (also shown in Figure 3), and the black line encompasses the California Region basin.

radiation into direct and diffuse components (Dingman 2002) and then corrects the direct component based on fields derived from the digital elevation model. This method has been shown to improve the simulation of the snowpack, especially during accumulation and melting periods (Kumar et al. 2013), which is critical when using a model simulation to inform water resources management decisions. Other fields (surface temperature, surface pressure, downward longwave radiation, and relative humidity) were downscaled using the standard atmospheric lapse rate (6.5 K/km) to adjust for differences between the 0.01° WLDAS model grid topography and the NLDAS-2 grid topography. Examples of the finer-scale spatial details of downscaled precipitation and downward shortwave radiation in mountainous regions are shown in Figure 3.

### *Data Assimilation*

Because of the importance of agriculture to the water and energy budgets in California and the stakeholders' desire for ET data, data assimilation (DA) of leaf area index (LAI) was implemented over the California Basin (2-digit hydrologic unit code [HUC] 18), a subregion of the WLDAS domain, in order to constrain the trajectory of the dynamic vegetation parameterization within Noah-MP. LAI is the ratio of the one-sided surface area of the vegetation canopy to the area of ground; therefore, larger numbers represent denser vegetation. As in Kumar, Mocko, et al. (2019), the one-dimensional ensemble Kalman filter (EnKF; Reichle et al. 2002) within LIS was applied to the state vector of simulated LAI; the updated LAI was also used to update the prognostic leaf biomass variable of the vegetation physics using the LSM's physics formulations. The simulation used 20 ensemble members. The Global LAnd Surface Satellite (GLASS) LAI product (Xiao et al. 2016) was used in this simulation and is available at eight-day intervals on a 0.05° × 0.05° grid for the period 1981–-present, though this simulation was run from 2000 to 2017, which is the period of the MODIS-based GLASS data. A limitation of using this product is that any disturbance or change to the vegetation must be large and persistent enough to be captured in the 0.05° eight-day data. It is expected that assimilating this product will capture large-scale phenomena (the overall growing season; droughts) rather

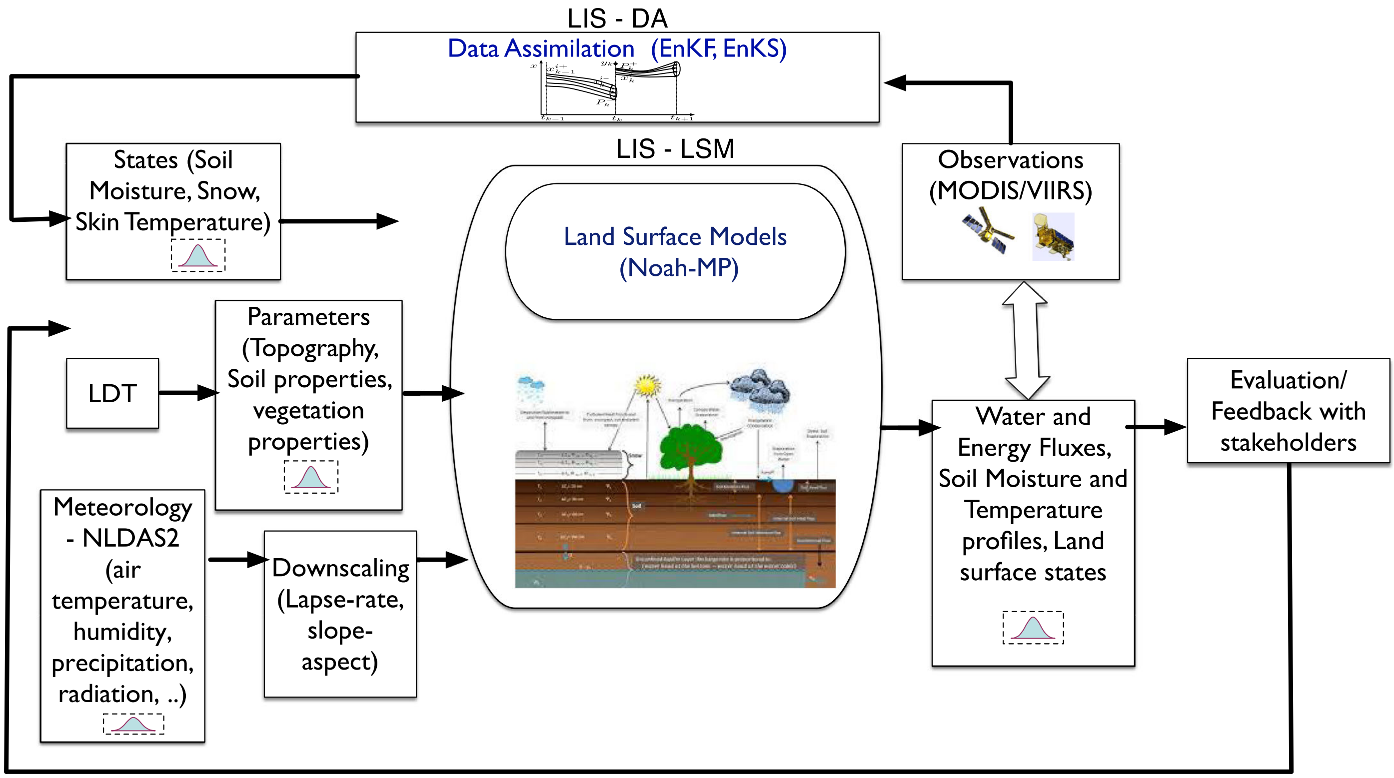


FIGURE 2. WLDAS product generation process. Parameters are processed with the Land Data Toolkit (LDT), and evaluation is conducted in part with the Land Verification Toolkit. LIS, Land Information System; DA, data assimilation; LSM, land surface model.

than finer-scale or fleeting features (harvesting or irrigating a small area). The eight-day observations were linearly interpolated to a daily frequency. Assimilation of this LAI product has been shown to improve Noah-MP estimation of multiple elements of the water budget (soil moisture, snow depth, streamflow, and ET), especially over agricultural areas (Kumar, Mocko, et al. 2019) at coarser 0.125° grid spacing.

In future versions of WLDAS, assimilation of Soil Moisture Active Passive (SMAP) soil moisture (O'Neill et al. 2016), including a newly developed 1-km SMAP soil moisture product (Fang et al. 2020; Liu et al. 2021, in revision), and Gravity Recovery and Climate Experiment (GRACE; Tapley et al. 2004) and GRACE Follow On terrestrial water storage (TWS) will be included.

## RESULTS: EVALUATION AND APPLICATIONS

### *Model Evaluation*

A retrospective open loop (OL) simulation of the daily water and energy budgets for the WLDAS domain was completed for 1979–2017. Outputs of the model (Table 3) include soil moisture, snow depth, SWE, ET, and soil temperature. Anomalies of the state variables are subsequently derived. The data are available in netCDF format at https://portal.nccs.nasa.gov/datashare/WLDAS/.

The performance of WLDAS was evaluated using LVT in comparison with the NLDAS-2 models (Xia et al. 2012) and the NLDAS Testbed models (Xia et al. 2017). The NLDAS-2 LSMs include Noah (Ek et al. 2003), Variable Infiltration Capacity (VIC; Liang et al. 1994), Mosaic (Koster and Suarez 1996), and Sacramento (SAC; Burnash et al. 1973). The NLDAS Testbed models include Noah-MP and the Catchment LSM (CLSM; Koster et al. 2000). For this analysis, the 0.01° WLDAS output was upscaled to 0.125° to facilitate a fairer comparison with the other models, rather than introducing additional uncertainties by downscaling the NLDAS-2 and Testbed output. However, the statistics for the finer scale 0.01° run are also included (denoted WLDAS 0.01 and WLDAS 0.125 in figures). The performance of each model's simulations of soil moisture was assessed using the International Soil Moisture Network (ISMN; Dorigo et al. 2011) stations. ET was evaluated using Atmosphere-Land Exchange Inverse (ALEXI; Anderson et al. 2007). Snow depth was

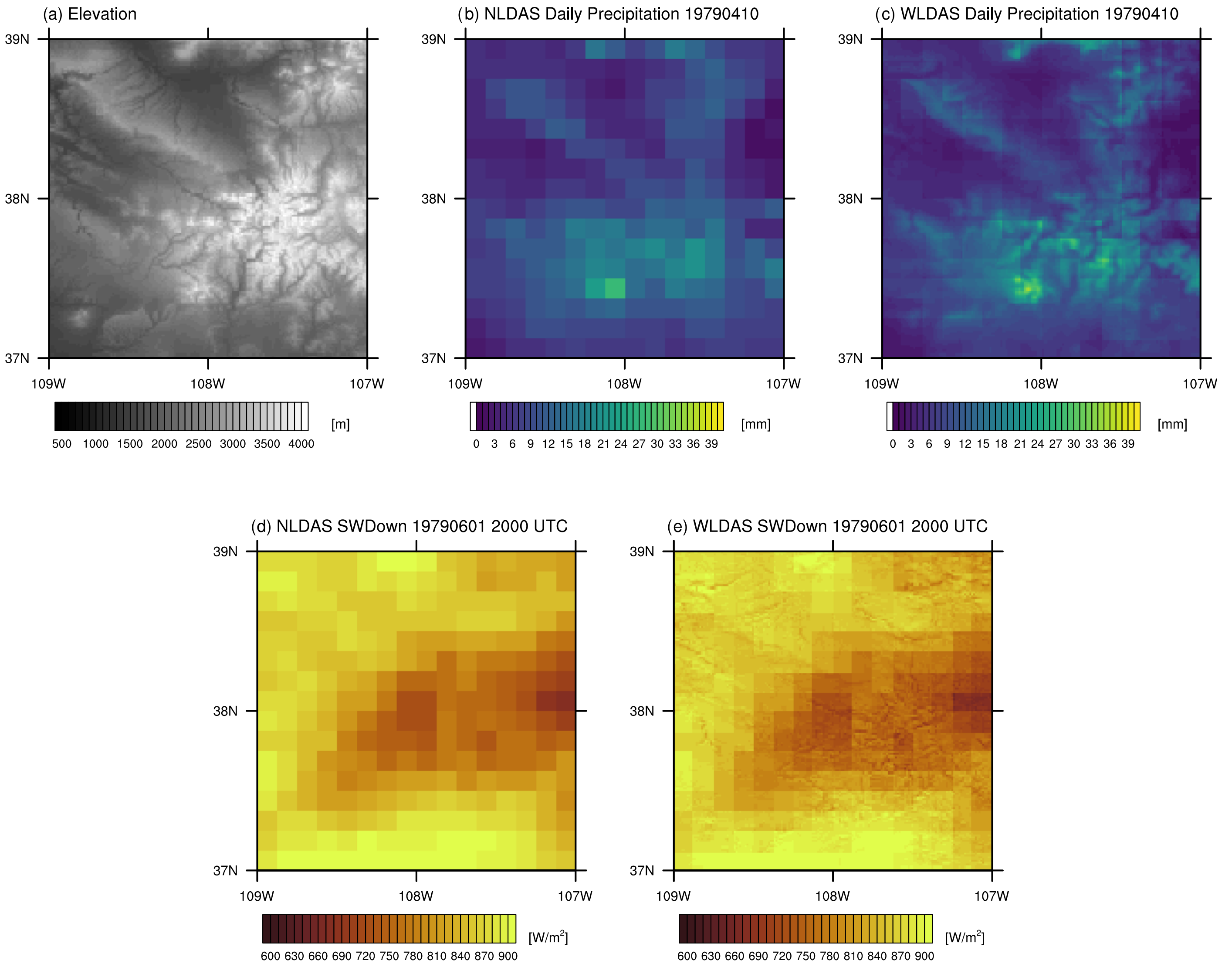


FIGURE 3. (a) Elevation, (b) North American Land Data Assimilation System (NLDAS) accumulated daily precipitation on 10 April 1979, (c) Downscaled WLDAS accumulated daily precipitation on 10 April 1979, (d) NLDAS downward shortwave radiation at 2000 UTC on 1 June 1979, and (e) Downscaled WLDAS downward shortwave radiation for 1 June 1979 for the region encompassed by the yellow box in Figure 1.

evaluated using the NOAA National Weather Service's National Operational Hydrologic Remote Sensing Center Snow Data Assimilation System (SNODAS; Barrett 2003) 1-km daily product. ET and snow depth were assessed using root mean square error (RMSE). Box plots describing the distribution of metrics for each product are presented in Figure 4.

The models do a reasonable job of capturing the components of the water budget. The soil moisture simulation in the products using Noah-MP (WLDAS and the NLDAS testbed version of Noah-MP) outperform the Noah model in NLDAS-2. However, they perform slightly worse than Noah in terms of ET, perhaps due to deficiencies in the dynamic vegetation model. These differences are statistically significant when using a *t*-test. It should be noted that model performance for these models is degraded when only considering the WLDAS domain as compared with other studies, which highlights the challenges of land surface modeling in areas of complex terrain (e.g., Kumar, Jasinski, et al. 2019). Many of these models perform better over the eastern U.S., which is reflected in the CONUS-wide scores.

Because of the importance of the snowpack to water resources managers in the western U.S., additional comparisons to snow observations were conducted. SWE was evaluated with a 4-km gridded SWE product developed at the University of Arizona (UASNOW; Zeng et al. 2018; Broxton et al. 2019) for water years from 1981 to 2017 and point-based Snow Telemetry (SNOTEL) sensors from 2010 to 2017 (The UASNOW product contains SNOTEL data.). The

Kling–Gupta efficiency (KGE; Gupta et al. 2009) is calculated as:

$$\mathrm{KGE} = 1 - \sqrt{(r-1)^2 + \left(\frac{\sigma_{\mathrm{sim}}}{\sigma_{\mathrm{obs}}} - 1\right)^2 + \left(\frac{\mu_{\mathrm{sim}}}{\mu_{\mathrm{obs}}} - 1\right)^2}, \tag{1}$$

where $r$ is correlation, $\sigma_{\mathrm{sim}}$ is the standard deviation of the model, $\sigma_{\mathrm{obs}}$ is the standard deviation of the observations, $\mu_{\mathrm{sim}}$ is the mean of the model, and $\mu_{\mathrm{obs}}$ is the mean of observed values. A perfect score of KGE is 1, and a value $<-0.41$ signifies that the mean of the observations performs better than the model timeseries.

When compared against the spatially gridded SWE product, WLDAS performs well in the mountainous areas west of 104°W (Figure 5). It is outperformed by the current version of VIC in NLDAS-2 in southwestern Wyoming, Utah, and in south-central Colorado. Mosaic performs better across the northern Great Plains, and Noah performs better in parts of Nebraska, Wyoming, and Montana as well. SAC KGE is better over much of the Plains. (see Figure S1 for a difference plot.) However, there is a marked improvement of the Noah-MP-based models over the other models in Washington, Oregon, California, Idaho, and Montana.

Similar patterns are also seen when comparing the performance of the models to SNOTEL observations (Figure 6; Figure S2). WLDAS generally shows improved performance over the NLDAS-2 models (Noah, VIC, Mosaic, SAC) in Washington, Oregon, and California, but is outperformed by VIC, SAC, and Mosaic in central Utah.

TABLE 3. Daily average output of the following variables is provided by WLDAS on a 0.01° × 0.01° grid. Bolded fields denote that the variable is available at multiple soil levels (0–10 cm, 10–40 cm, 40–100 cm, and 100–200 cm below the surface)

| Variable | Units |
|---|---|
| **Soil moisture** | **$m^3/m^3$** |
| **Soil temperature** | **K** |
| Snowmelt | $kg/m^2/s$ |
| Snow water equivalent | $kg/m^2/s$ |
| Snow depth | m |
| Snow sublimation | $kg/m^2/s$ |
| Snow cover fraction | — |
| Evapotranspiration (ET) | $kg/m^2/s$ |
| Interception evaporation | $kg/m^2/s$ |
| Vegetation transpiration | $kg/m^2/s$ |
| Bare soil evaporation | $kg/m^2/s$ |
| Total canopy water storage | $kg/m^2/s$ |
| Surface runoff | $kg/m^2/s$ |
| Subsurface runoff | $kg/m^2/s$ |
| Net downward longwave flux | $W/m^2$ |
| Net downward shortwave flux | $W/m^2$ |
| Upward latent heat flux | $W/m^2$ |
| Upward sensible heat flux | $W/m^2$ |
| Downward heat flux in soil | $W/m^2$ |
| Snowfall rate | $kg/m^2/s$ |
| Precipitation rate | $kg/m^2/s$ |
| Canopy temperature | K |
| Bare soil temperature | K |
| Surface temperature | K |
| Surface radiative temperature | K |
| Water table depth | m |
| Terrestrial water storage (TWS) | mm |
| Groundwater storage | mm |
| Wind speed | m/s |
| Total precipitation rate (rain + snow) | $kg/m^2/s$ |
| Air temperature | K |
| Specific humidity | kg/kg |
| Surface pressure | Pa |
| Surface downward shortwave radiation | $W/m^2$ |
| Surface downward longwave radiation | $W/m^2$ |
| Water in aquifer and saturated soil | mm |

### *WLDAS Applications*

State variables such as soil moisture and temperature, SWE, snow depth, runoff, and ET are native outputs of WLDAS (Table 3). The length of the WLDAS record and the number of variables produced by the system also allow for the computation of derived quantities that are valuable to stakeholders. Because of the long simulation time, percentiles and anomalies of state variables can be computed, contextualizing hydrological conditions. Additionally, these variables can be combined to produce additional variables, such as groundwater recharge.

**Groundwater Recharge.** A key deliverable of the WLDAS dataset is a timeseries of natural groundwater recharge (Li et al. 2021). This product represents diffuse recharge (i.e., the water flowing into aquifers through downward moisture flux in the soil column, as opposed to recharge beneath surface water features and macropore flows), and is mainly driven by precipitation and snowmelt. Recharge is computed from WLDAS outputs as:

$$\text{recharge} = \text{groundwater storage change} + \text{baseflow}, \tag{2}$$

where baseflow (also known as subsurface runoff in Noah-MP) is defined as discharge to rivers and streams. The groundwater storage change was calculated between two consecutive days due to the daily output frequency in WLDAS.

For stakeholders, WLDAS recharge represents the expected amount of natural input to aquifers, ignoring lateral flows, subsurface heterogeneity, preferential flow paths, and anthropogenic contributions (injections and irrigation return flows). These

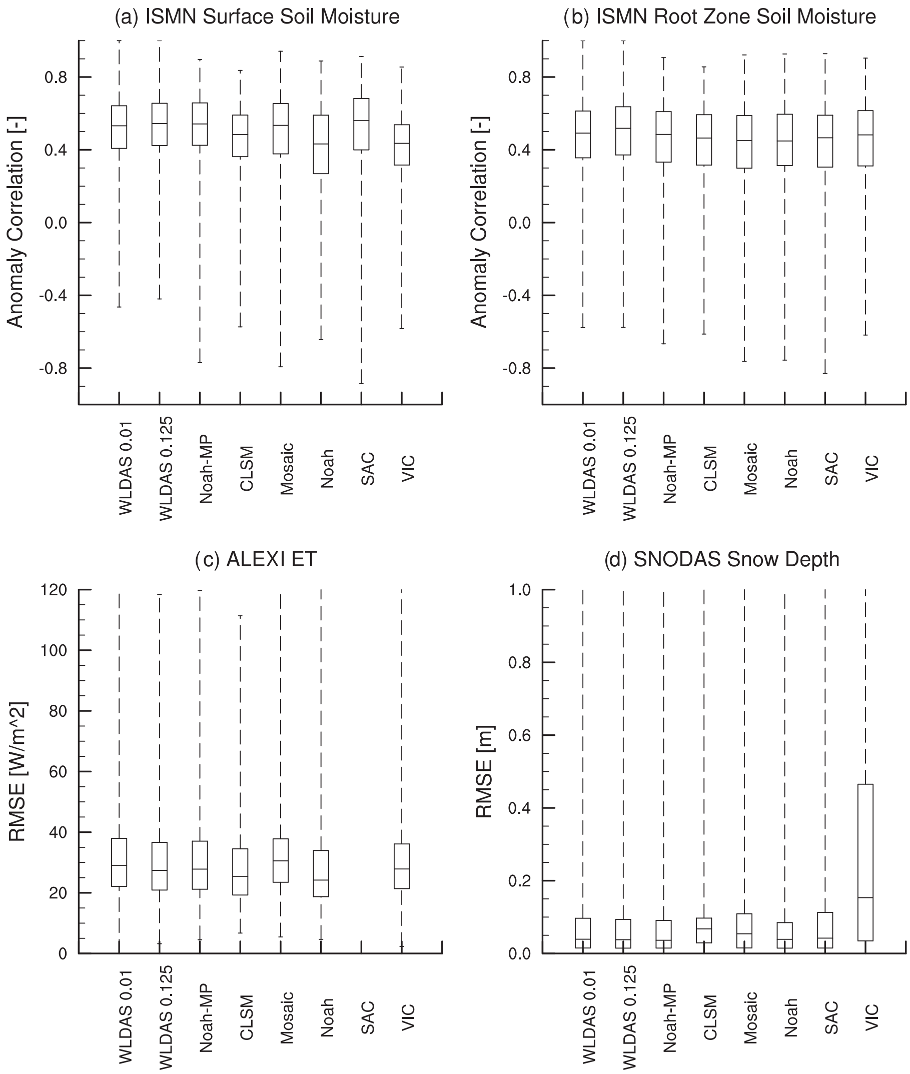


FIGURE 4. Boxplots of anomaly correlation for soil moisture based on the International Soil Moisture Network for (a) surface soil moisture and (b) root zone soil moisture. Root mean square error (RMSE) for (c) Atmosphere-Land Exchange Inverse (ALEXI) ET and (d) Snow Data Assimilation System (SNODAS) snow depth. ISMN, International Soil Moisture Network; CLSM, Catchment LSM; SAC, Sacramento; VIC, Variable Infiltration Capacity.

limitations are discussed more fully in Li et al. (2021). The climatology of WLDAS groundwater recharge is shown in Figure 7. This simulated diffuse recharge may be used as an input at the upper boundary of a groundwater flow model. Over California, diffuse recharge mainly occurs from December to April, which coincides with the maximum in precipitation over the region and illustrates the control of ET in reducing recharge to aquifers in the warm season (Li et al. 2021).

**Drought Detection and Monitoring.** A strength of WLDAS is its relatively long record, which allows users to place present hydrological events in a historical context. Tools for these applications include percentile and anomaly information, both of which can be calculated in LVT. For example, WLDAS captures the severity of the recent California drought. TWS and root zone (0–1 m below ground) soil moisture (RZSM) percentiles were calculated for each day, using a five-day moving average of the calendar day ±2 days. Therefore, the percentile values for May 20 would be based on the values from May 18 to 22 over the entire simulation. These percentiles can be used to generate simulated drought indices (e.g., Houborg et al. 2012; Li et al. 2019). TWS represents the total amount of water in each pixel including soil water, surface water, groundwater storage, and the snowpack and serves as an integrated measure of hydrological conditions. Figure 8 shows the percentage of the HUC 18 basin shown in Figure 2 that is below a certain RZSM and TWS percentile for

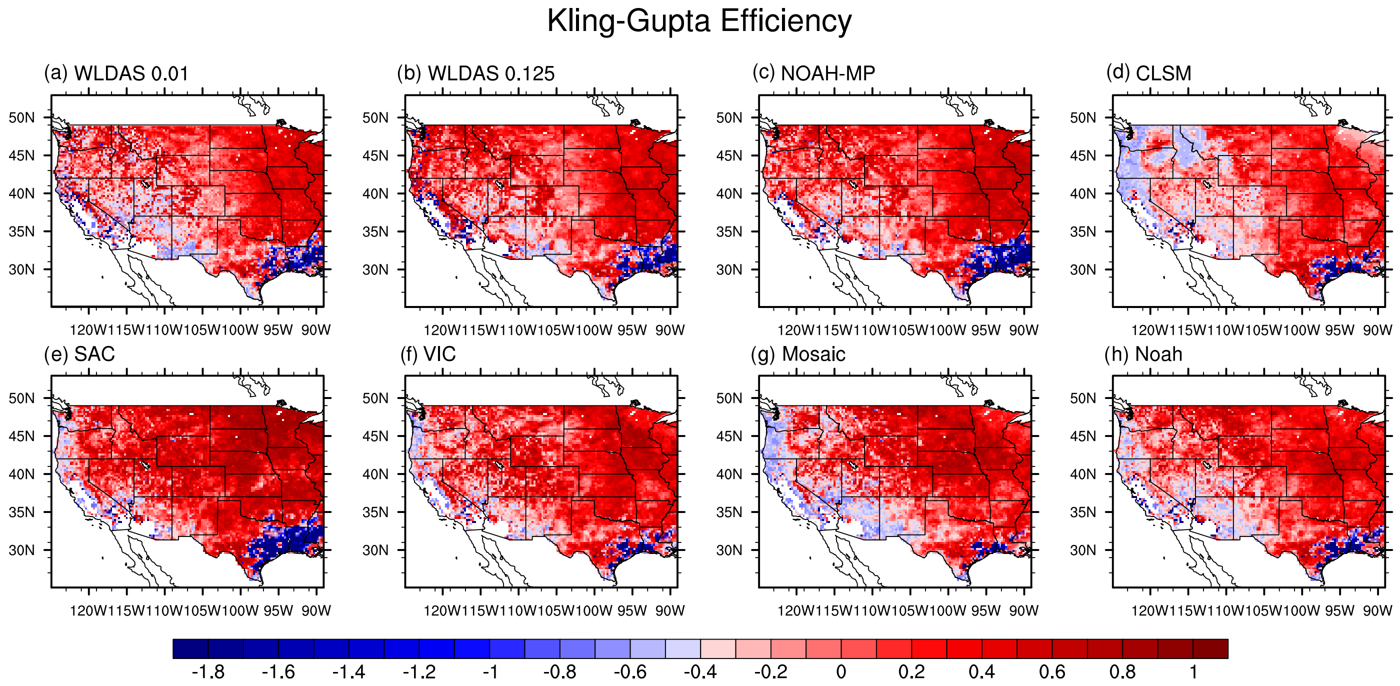


FIGURE 5. Kling–Gupta efficiency (KGE) of modeled snow water equivalent (SWE) vs. UASNOW SWE during water years 1981–2017 for (a) WLDAS 0.01°, (b) WLDAS 0.125°, (c) Noah-MP, (d) CLSM, (e) SAC, (f) VIC, (g) Mosaic, and (h) Noah.

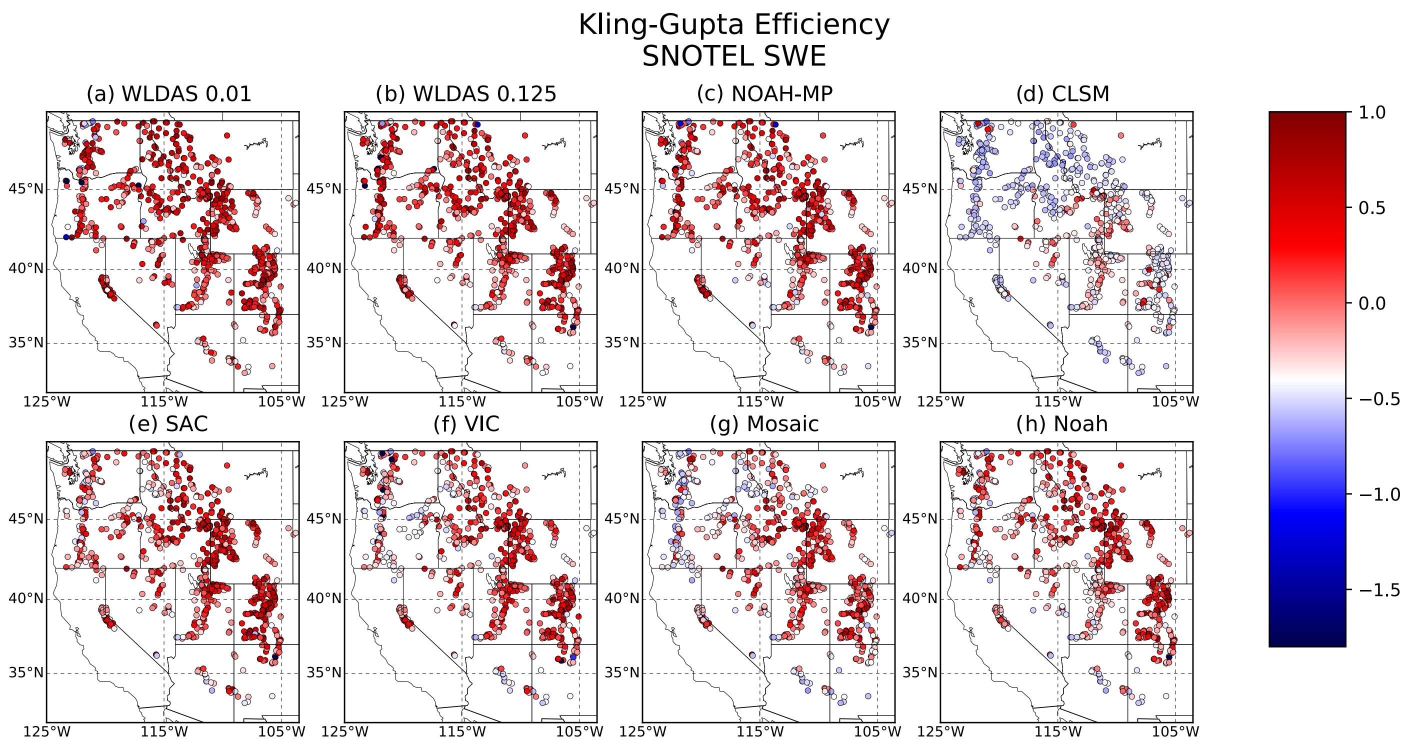


FIGURE 6. KGE of modeled SWE vs. Snow Telemetry SWE during 2010–2017 for (a) WLDAS 0.01°, (b) WLDAS 0.125°, (c) Noah-MP, (d) CLSM, (e) SAC, (f) VIC, (g) Mosaic, and (h) Noah.

2000–2017. According to WLDAS, almost the entire basin was below the 30th percentile for soil moisture and TWS on 1 January 2014, with nearly 60% of the basin area at or below the 2nd percentile. The dry conditions persisted with a slight decrease in the area affected in 2016. Most of the basin had recovered by

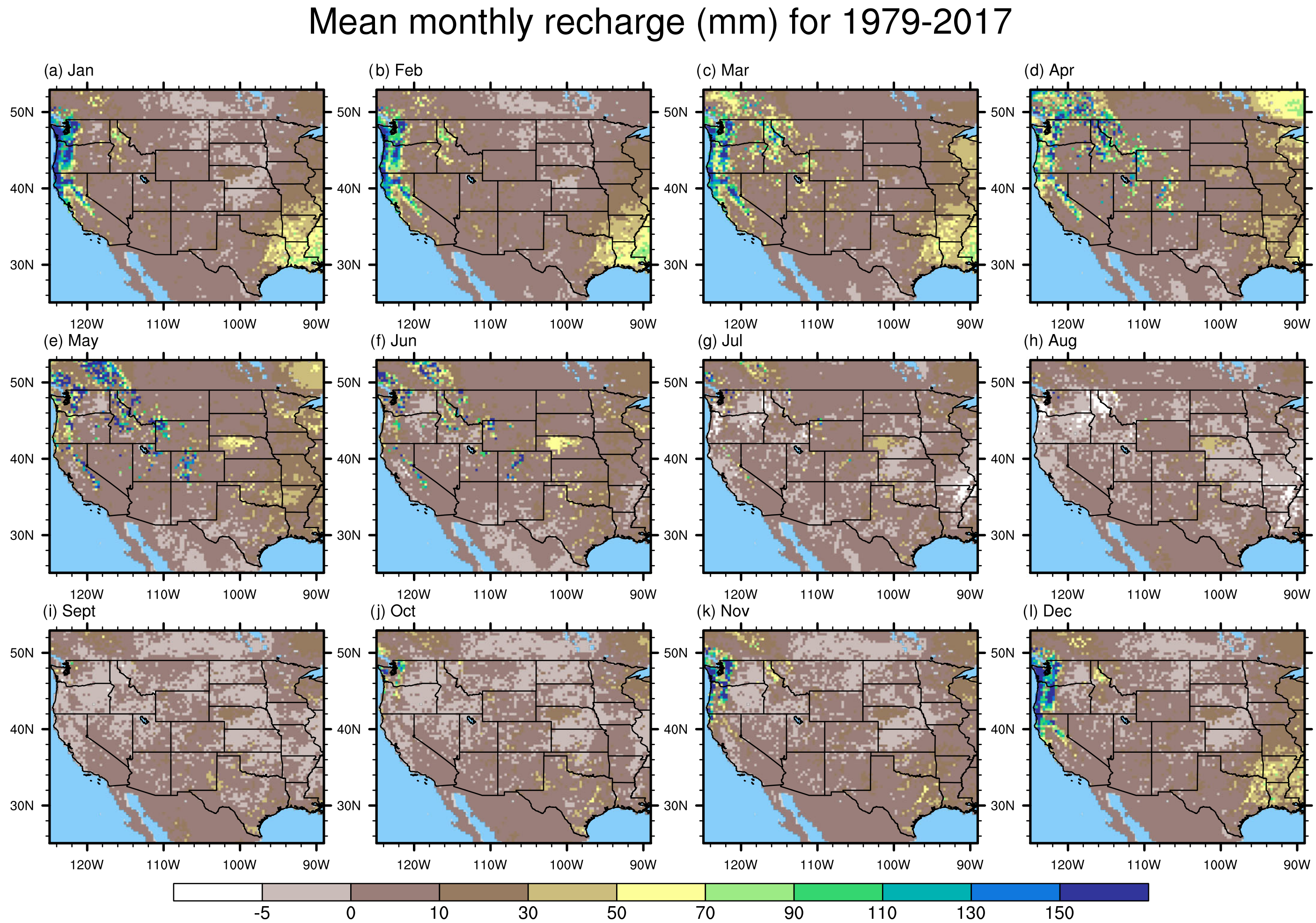


FIGURE 7. Seasonal cycle of mean recharge.

2017. The U.S. Drought Monitor (USDM; Svoboda et al. 2002) is also shown for reference. The USDM is authored by the National Drought Mitigation Center, the National Oceanic and Atmospheric Administration, and the U.S. Department of Agriculture. The authors consider a number of drought and precipitation indices and other variables such as vegetation, snowpack, streamflow, and soil moisture. The time-series from WLDAS offer another product for the USDM authors to use when creating their maps.

Figure 9 shows spatial maps of the recent drought-to-flood transition over the state of California. The drought is captured by both the RZSM and TWS percentiles in WLDAS and in the 0.125° GRACE-based shallow groundwater drought indicators (DI; Houborg et al. 2012; available at https://nasagrace.unl.edu). The modeled estimates generally match the USDM spatial pattern well. WLDAS has a higher spatial resolution (1-km) than both the USDM (hand-drawn based largely on county-level and 0.125° resolution data) and the GRACE-based DI (0.125°). When considering factors other than soil moisture, the drought in WLDAS is more severe in TWS in 2015 in the mountains (panels d, j, k, and v), when the snowpack is almost nonexistent. The shallow groundwater GRACE-based DI also indicates greater severity in the mountains. By late 2016, much of the basin had transitioned into a period of high TWS (panels e, k, q, and w). However, the low TWS (panel l) and shallow groundwater (panel r) percentiles lingered in southern California, even after much of the state had recovered. By examining percentiles for variables other than soil moisture or by considering integrated measures such as TWS, the WLDAS end users can characterize abnormal conditions in the entire column.

**Impact of Data Assimilation.** In order to improve the estimation of ET within WLDAS, LAI DA was enabled over California as a testbed for future improvements to WLDAS. Successful enhancements will be applied to the full domain in the future.

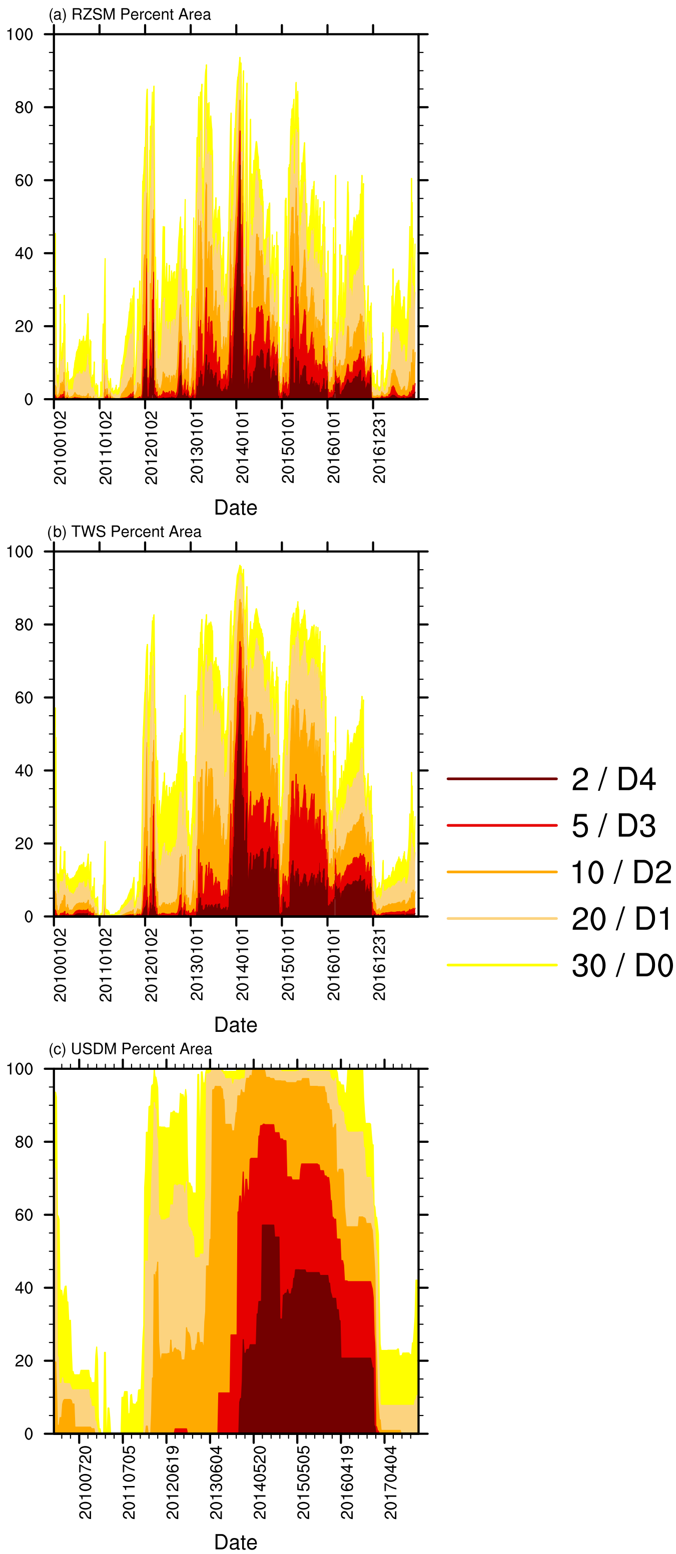


FIGURE 8. Daily percent area of the California watershed in Figure 1 below a given percentile for (a) root zone (0–1 m below surface) soil moisture, (b) TWS, and (c) United States Drought Monitor (USDM). RZSM, root zone soil moisture.

The impact of including LAI assimilation in the model was compared against four satellite-based ET products: ALEXI, Global Land surface Evaporation: the Amsterdam Methodology (GLEAM; Miralles et al. 2011), University of Washington (UW; Tang et al. 2009), and FLUXNET Multi-Tree Ensemble (MTE; Jung et al. 2009). Each of these products estimates ET using a different approach over a different time period, and the accuracy of the satellite-based products is dependent on point calibration against a subset of the FLUXNET observations, so this exercise is an intercomparison among products rather than against a measure of ground truth. ALEXI uses land surface temperature obtained from geostationary satellites and is available at 4-km and daily resolution from 2001 to 2015. GLEAM is based on a Priestly-Taylor evaporation model whose inputs are primarily from passive microwave sensors (available at 0.25° at daily timescales from 1980 to 2014). The UW product uses MODIS products and the National Oceanic and Atmospheric Administration National Environmental Satellite, Data, and Information Service surface radiation budget to provide monthly (2001–2008), 5-km estimates of ET. FLUXNET-MTE data are upscaled to a 0.25° grid from FLUXNET eddy covariance towers (available daily from 1982 to 2008).

Correlation, RMSE, and KGE were the metrics chosen to evaluate the performance of the LAI assimilation compared to the OL run, which did not have DA enabled. Maps of the difference in metrics between the two simulations (DA minus OL) are shown in Figures 10 and 11. The DA runs over California showed an improvement in ET over agricultural areas in California when compared with ALEXI, UW, and FLUXNET MTE data. In pixels that showed improvements (positive difference in correlation; negative difference in RMSE), the RMSE improvements were greatest for evaluation using FLUXNET (2.875 $W/m^2$) followed by UW (2.441 $W/m^2$), ALEXI (2.135 $W/m^2$), and GLEAM (1.301 $W/m^2$). Evaluation using UW had the most favorable average increase in correlation (0.104), followed by FLUXNET (0.099), ALEXI (0.074), and GLEAM (0.038). KGE also improved over the Central Valley (Figure 12) when compared to UW, ALEXI, and FLUXNET data. The areas of large improvement in the north coincide with areas where rice and deciduous trees and nuts are grown (CDWR 2019). These improvements show strong seasonality and are the largest over the Central Valley during June-September (Figure 13), coinciding with the growing season. The seasonality of improvement in the Central Valley was also seen in the FLUXNET and UW data (not shown). This is logical considering that WLDAS does not yet

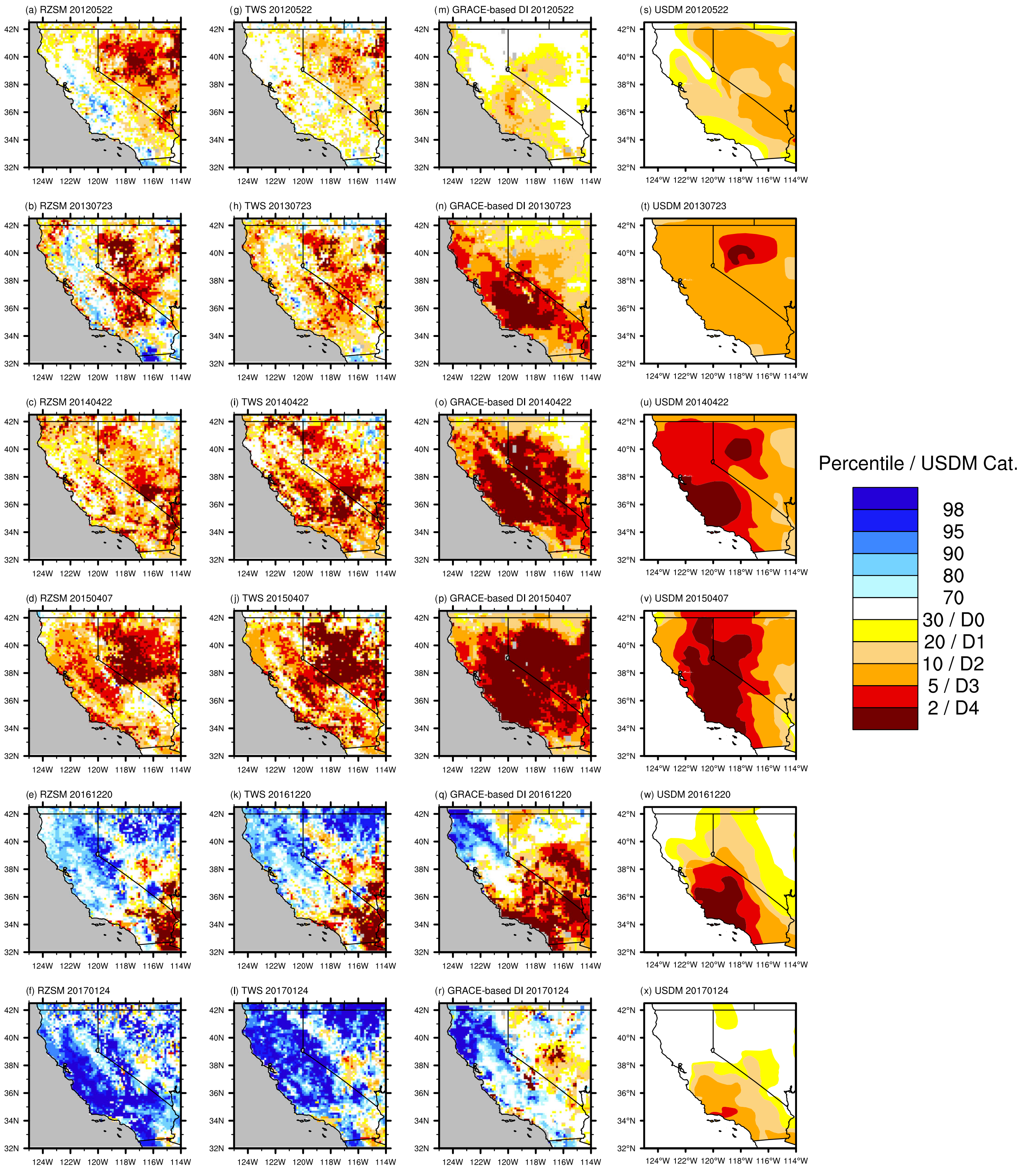


FIGURE 9. WLDAS root zone soil moisture percentiles (first column; a–f), WLDAS TWS percentiles (second column; g–l), GRACE-based shallow groundwater drought indicators (third column; m–r), and USDM (fourth column; s–x) for 22 May 2012, 23 July 2013, 22 April 2014, 7 April 2015, 20 December 2016, and 24 January 2017.

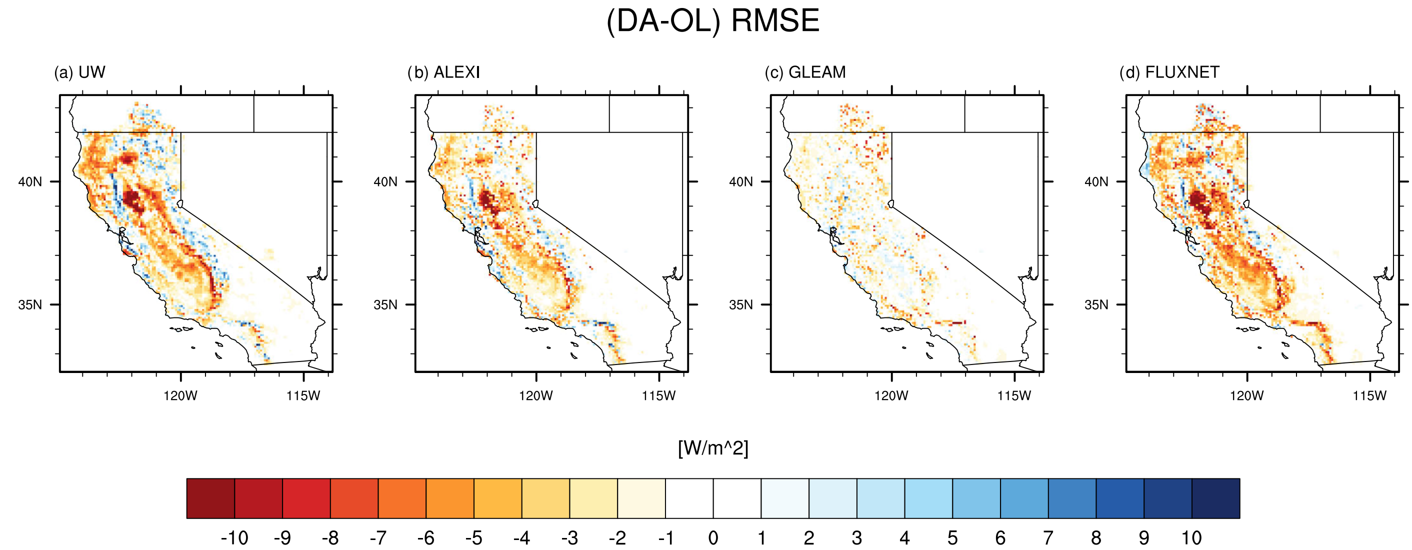


FIGURE 10. Differences in RMSE between the LAI DA run and the open loop run over California using (a) University of Washington (UW; 2002–2012) (b) ALEXI (2002–2015) (c) Global Land surface Evaporation: the Amsterdam Methodology (GLEAM; 2000–2017), and (d) FLUXNET (2000–2009) ET for evaluation. Warm colors indicate improvements. OL, Open Loop.

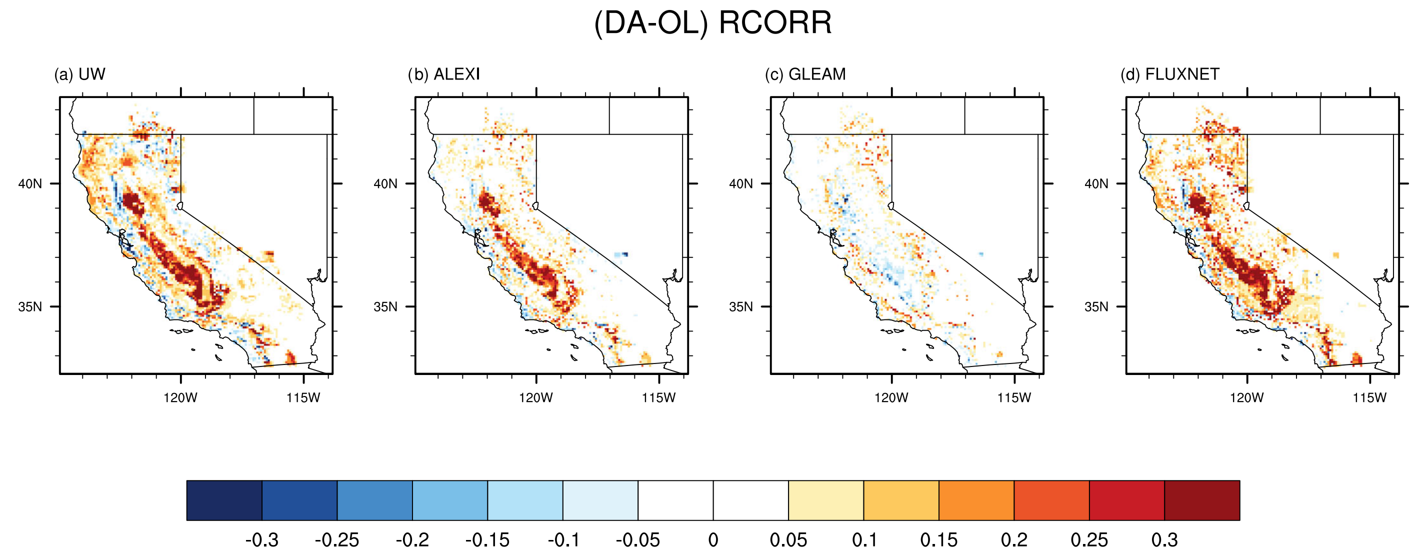


FIGURE 11. Differences in correlation between the LAI DA run and the open loop run over California using (a) UW (2002–2012) (b) ALEXI (2002–2015) (c) GLEAM (2000–2017), and (d) FLUXNET (2000–2009) ET for evaluation. Warm colors indicate improvements.

simulate irrigation and crop growth, so that there is the largest potential for improvement in simulating ET over agricultural regions.

## SUMMARY AND CONCLUSIONS

WLDAS, a high-resolution instance of LIS and the associated output dataset, was run over the western U.S. to support water resources decision-making including sustainable groundwater management. The WLDAS products have a wide range of potential applications including water budget assessment, drought quantification, crop yield forecasting, and groundwater sustainable use planning. The downscaled forcing data are also publicly available. WLDAS spans a long record (1979–present), which is crucial for contextualizing events using derived metrics such as wetness anomalies and percentiles. Stakeholders including our partners at the California SWRBC specifically requested information characterizing the expected

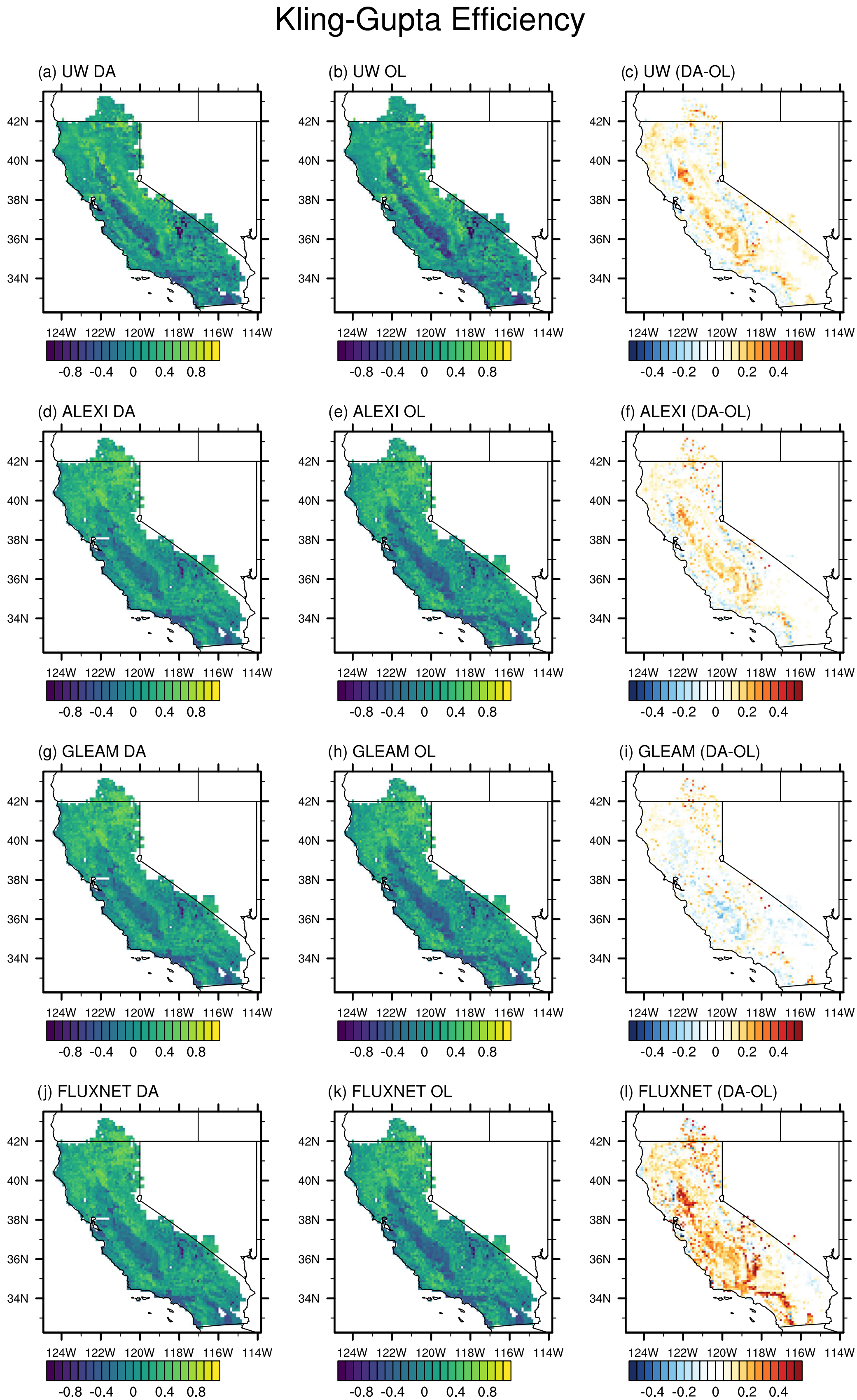


FIGURE 12. KGE and difference in KGE (DA-OL) for UW (a–c), ALEXI (d–f), GLEAM (g–i), and FLUXNET (j–l) ET.

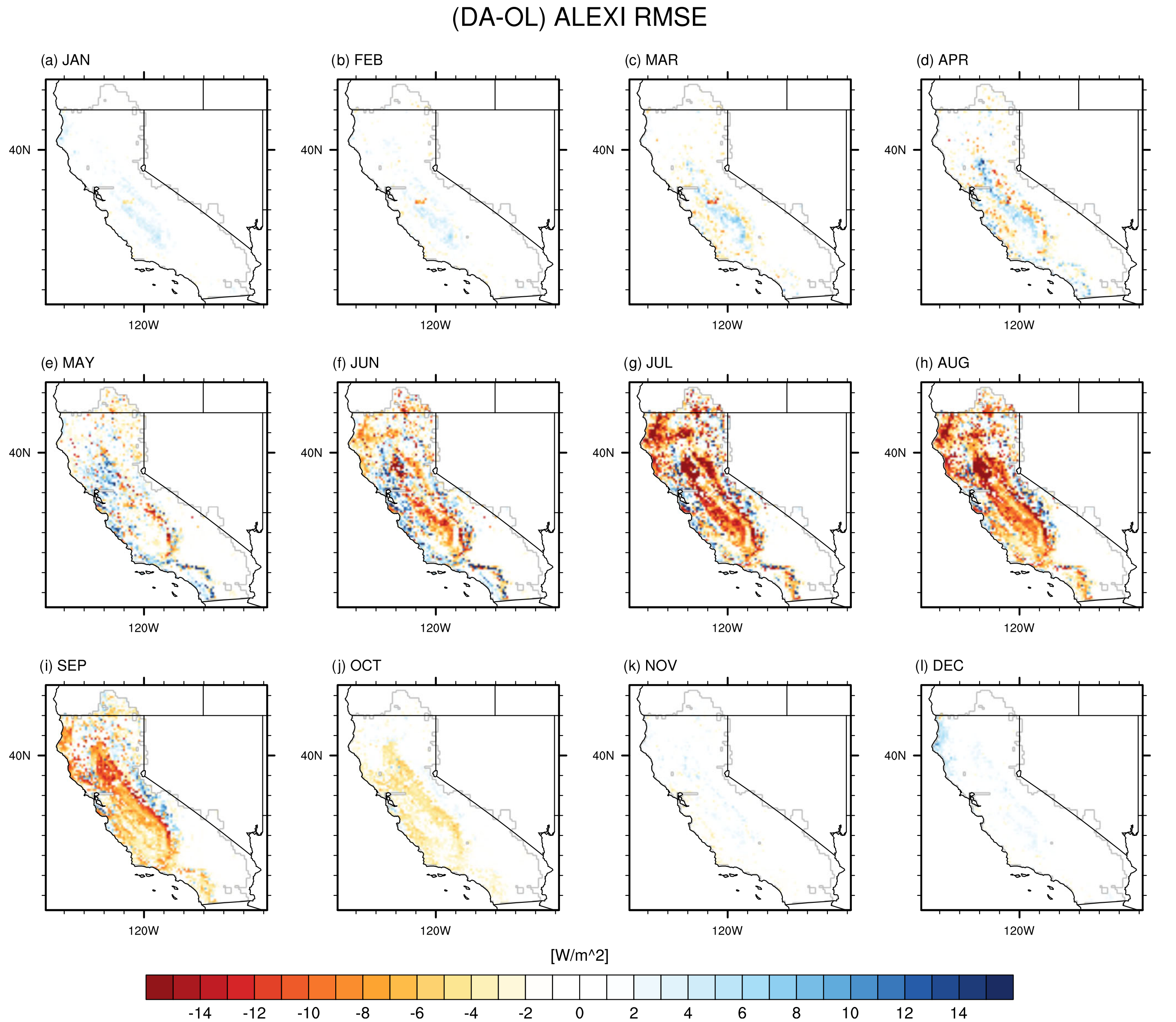


FIGURE 13. Monthly differences (DA-OL) in ET based on ALEXI data for (a) January, (b) February, (c) March, (d) April, (e) May, (f) June, (g) July, (h) August, (i) September, (j) October, (k) Novembver, and (l) December. Warm colors indicate an improvement when using DA.

recharge to aquifers from precipitation and snowmelt, and such a product has been derived from the WLDAS output.

The performance of WLDAS was evaluated in comparison to the existing NLDAS-2 suite of products and the NLDAS Testbed models and was found to perform similarly to other products that use the same base LSM. As part of WLDAS development, changes to the OL reanalysis were explored, including the addition of satellite DA. Over California, the assimilation of LAI was shown to improve the model's estimation of ET by constraining the dynamic vegetation model within Noah-MP. The largest improvements occurred over agricultural areas during the warm season. As one example, WLDAS captures the evolution of the historic 2011–2017 drought in California in both the RZSM and TWS percentiles and provides a higher resolution spatial pattern of the drought when compared to existing GRACE-based drought indications and the USDM.

Additional planned enhancements to WLDAS include enabling GRACE and GRACE Follow on TWS and SMAP soil moisture DA features in LIS (Kumar et al. 2016; Kumar, Jasinski, et al. 2019) as well as the irrigation simulation routine introduced by Ozdogan et al. (2010). Future development will involve WLDAS optimization to support the needs of additional partners throughout the western U.S., specifically in Colorado, and will focus on drought assessment, improvement of meteorological forcing using local data, irrigation, and other needs that arise from stakeholders.

## SUPPORTING INFORMATION

Additional supporting information may be found online under the Supporting Information tab for this article: Difference plots for Figure 5 and Figure 6.

### ACKNOWLEDGMENTS

WLDAS is supported by NASA's Applied Sciences Program and the Western Water Applications Office. Model simulations and evaluations were conducted using the NASA Center for Climate Simulation (NCCS) at Goddard Space Flight Center. The NLDAS-2 forcing data used in this effort were acquired as part of the activities of NASA's Science Mission Directorate and are archived and distributed by the Goddard Earth Sciences (GES) Data and Information Services Center (DISC). A portion of this research was carried out at the Jet Propulsion Laboratory, California Institute of Technology, under a contract with the National Aeronautics and Space Administration (80NM0018D0004).

## AUTHORS' CONTRIBUTIONS

**Jessica M. Erlingis:** Data curation; formal analysis; investigation; methodology; validation; visualization; writing-original draft; writing-review & editing. **Matt Rodell:** Conceptualization; funding acquisition; methodology; supervision; writing-review & editing. **Christa D. Peters-Lidard:** Conceptualization; funding acquisition; methodology; supervision. **Bailing Li:** Data curation; formal analysis; investigation; methodology; writing-review & editing. **Sujay V. Kumar:** Conceptualization; funding acquisition; methodology; software; supervision; writing-review & editing. **James S. Famiglietti:** Conceptualization; project administration. **Stephanie L. Granger:** Project administration. **John V. Hurley:** Methodology; writing-review & editing. **Pang-Wei Liu:** Investigation; writing-review & editing. **David M. Mocko:** Validation; writing-review & editing.

### LITERATURE CITED

Anderson, M.C., J.M. Norman, J.R. Mecikalski, J.A. Otkin, and W.P. Kustas. 2007. "A Climatological Study of Evapotranspiration and Moisture Stress across the Continental United States Based on Thermal Remote Sensing: 1. Model Formulation." *Journal of Geophysical Research: Atmospheres* 112. https://doi.org/10.1029/2006JD007506.

Arsenault, K.R., S.V. Kumar, J.V. Geiger, S. Wang, E. Kemp, D.M. Mocko, H.K. Beaudoing *et al*. 2018. "The Land Surface Data Toolkit (LDT v7.2) — A Data Fusion Environment for Land Data Assimilation Systems." *Geoscientific Model Development* 11: 3605–21.

Baldwin, M.E., and K.E. Mitchell. 1997. "The NCEP Hourly Multisensor US Precipitation Analysis for Operations and GCIP Research." Preprints, 13th Conf. on Hydrology, Long Beach, CA, Amer. Meteor. Soc.

Ball, J.T., I.E. Woodrow, and J.A. Berry. 1987. "A Model Predicting Stomatal Conductance and Its Contribution to the Control of Photosynthesis under Different Environmental Conditions BT." In *Progress in Photosynthesis Research: Volume 4 Proceedings of the VIIth International Congress on Photosynthesis Providence, Rhode Island, USA, August 10–15, 1986*, edited by J. Biggins, 221–4.Dordrecht, The Netherlands: Springer.

Barrett, A. 2003. "National Operational Hydrologic Remote Sensing Center Snow Data Assimilation System (SNODAS) products at NSIDC." NSIDC Special Report 11: 19 pp.

Broxton, P., X. Zeng, and N. Dawson. 2019. *Daily 4 km Gridded SWE and Snow Depth from Assimilated In-Situ and Modeled Data over the Conterminous US, Version 1 [1981–2017]*. Boulder, CO: NASA National Snow and Ice Data Center Distributed Active Archive Center. https://doi.org/10.5067/0GGPB220EX6A.

Burnash, R.J.C., R.L. Ferral, and R.A. McGuire. 1973. "A Generalized Streamflow Simulation System: Conceptual Models for Digital Computers." Joint Federal and State River Forecast Center, U.S. National Weather Service and California Department of Water Resources Tech. Rep., 204 pp.

CDWR. 2019. "2016 California Statewide Agricultural Land Use." California Department of Water Resources. https://gis.water.ca.gov/app/CADWRLandUseViewer/.

Chen, M., W. Shi, P. Xie, V.B.S. Silva, V.E. Kousky, R. Wayne Higgins, and J.E. Janowiak. 2008. "Assessing Objective Techniques for Gauge-Based Analyses of Global Daily Precipitation." *Journal of Geophysical Research: Atmospheres* 113. https://doi.org/10.1029/2007JD009132.

Cosgrove, B.A., D. Lohmann, K.E. Mitchell, P.R. Houser, E.F. Wood, J.C. Schaake, A. Robock *et al*. 2003. "Real-Time and Retrospective Forcing in the North American Land Data Assimilation System (NLDAS) Project." *Journal of Geophysical Research: Atmospheres* 108. https://doi.org/10.1029/2002JD003118.

Daly, C., M. Halbleib, J.I. Smith, W.P. Gibson, M.K. Doggett, G.H. Taylor, J. Curtis, and P.P. Pasteris. 2008. "Physiographically Sensitive Mapping of Climatological Temperature and Precipitation across the Conterminous United States." *International Journal of Climatology* 28: 2031–64.

Dickinson, R.E., M. Shaikh, R. Bryant, and L. Graumlich. 1998. "Interactive Canopies for a Climate Model." *Journal of Climate* 11: 2823–36.

Dingman, S.L. 2002. *Physical Hydrology*. Upper Saddle River, NJ: Prentice Hall.

Dorigo, W., P. van Oevelen, W. Wagner, M. Drusch, S. Mecklenburg, A. Robock, and T. Jackson. 2011. "A New International Network for in Situ Soil Moisture Data." *Eos, Transactions American Geophysical Union* 92: 141–2.

Ek, M.B., K.E. Mitchell, Y. Lin, E. Rogers, P. Grunmann, V. Koren, G. Gayno, and J.D. Tarpley. 2003. "Implementation of Noah Land Surface Model Advances in the National Centers for Environmental Prediction Operational Mesoscale Eta Model." *Journal of Geophysical Research: Atmospheres* 108. https://doi.org/10.1029/2002JD003296.

Famiglietti, J.S. 2014. "The Global Groundwater Crisis." *Nature Climate Change* 4: 945–8.

Famiglietti, J.S., A. Cazenave, A. Eicker, J.T. Reager, M. Rodell, and I. Velicogna. 2015. "Satellites Provide the Big Picture." *Science* 349: 684–5.

Famiglietti, J.S., M. Lo, S.L. Ho, J. Bethune, K.J. Anderson, T.H. Syed, S.C. Swenson, C.R. de Linage, and M. Rodell. 2011. "Satellites Measure Recent Rates of Groundwater Depletion in California's Central Valley." *Geophysical Research Letters* 38. https://doi.org/10.1029/2010GL046442.

Fang, B., V. Lakshmi, R. Bindlish, T.J. Jackson, and P.-W. Liu. 2020. "Evaluation and Validation of a High Spatial Resolution Satellite Soil Moisture Product over the Continental United States." *Journal of Hydrology* 588: 125043.

Faunt, C.C., ed. 2009. "Groundwater Availability of the Central Valley Aquiver, California." U.S. Geological Survey Professional Paper 1766, 225 pp.

Funk, C., A. Hoell, and D. Stone. 2014. "Examining the Contribution of the Observed Global Warming Trend to the California Droughts of 2012/13 and 2013/14." *Bulletin of the American Meteorological Society* 95 (9): S11–15.

Giordano, M. 2009. "Global Groundwater? Issues and Solutions." *Annual Review of Environment and Resources* 34: 153–78.

Gleeson, T., Y. Wada, M.F.P. Bierkens, and L.P.H. van Beek. 2012. "Water Balance of Global Aquifers Revealed by Groundwater Footprint." *Nature* 488: 197–200.

Gupta, H.V., H. Kling, K.K. Yilmaz, and G.F. Martinez. 2009. "Decomposition of the Mean Squared Error and NSE Performance Criteria: Implications for Improving Hydrological Modelling." *Journal of Hydrology* 377: 80–91.

Harrison, K.W., S.V. Kumar, C.D. Peters-Lidard, and J.A. Santanello. 2012. "Quantifying the Change in Soil Moisture Modeling Uncertainty from Remote Sensing Observations Using Bayesian Inference Techniques." *Water Resources Research* 48. https://doi.org/10.1029/2012WR012337.

Herring, S.C., M.P. Hoerling, T.C. Peterson, and P.A. Stott. 2014. "Explaining Extreme Events of 2013 from a Climate Perspective." *Bulletin of the American Meteorological Society* 95: S1–S104.

Higgins, R.W., W. Shi, E. Yarosh, and R. Joyce. 2000. "Improved United States Precipitation Quality Control System and Analysis." NCEP/Climate Prediction Center Atlas 7: 40 pp.

Houborg, R., M. Rodell, B. Li, R. Reichle, and B.F. Zaitchik. 2012. "Drought Indicators Based on Model-Assimilated Gravity Recovery and Climate Experiment (GRACE) Terrestrial Water Storage Observations." *Water Resources Research* 48. https://doi.org/10.1029/2011WR011291.

Jasinski, M.F., J.S. Borak, S.V. Kumar, D.M. Mocko, C.D. Peters-Lidard, M. Rodell, H. Rui *et al*. 2019. "NCA-LDAS: Overview and Analysis of Hydrologic Trends for the National Climate Assessment." *Journal of Hydrometeorology* 20: 1595–617.

Jordan, R. 1991. "A One-Dimensional Temperature Model for a Snow Cover: Technical Documentation for SNTERERM.90." Special Rep. 91-16, Cold Region Research and Engineers Laboratory, U.S. Army Corps of Engineers, Hanover, NH, 61 pp.

Joyce, R.J., J.E. Janowiak, P.A. Arkin, and P. Xie. 2004. "CMORPH: A Method That Produces Global Precipitation Estimates from Passive Microwave and Infrared Data at High Spatial and Temporal Resolution." *Journal of Hydrometeorology* 5: 487–503.

Jung, M., M. Reichstein, and A. Bondeau. 2009. "Towards Global Empirical Upscaling of FLUXNET Eddy Covariance Observations: Validation of a Model Tree Ensemble Approach Using a Biosphere Model." *Biogeosciences* 6: 2001–13.

Koster, R., and M. Suarez. 1996. "Energy and Water Balance Calculations in the Mosaic LSM." NASA Tech. Memo, NASA, TM-104606 9, 60 pp.

Koster, R.D., M.J. Suarez, A. Ducharne, M. Stieglitz, and P. Kumar. 2000. "A Catchment-Based Approach to Modeling Land Surface Processes in a General Circulation Model: 1. Model Structure." *Journal of Geophysical Research: Atmospheres* 105: 24809–22.

Kumar, S.V., M. Jasinski, D.M. Mocko, M. Rodell, J. Borak, B. Li, H.K. Beaudoing, and C.D. Peters-Lidard. 2019a. "NCA-LDAS Land Analysis: Development and Performance of a Multisensor, Multivariate Land Data Assimilation System for the National Climate Assessment." *Journal of Hydrometeorology* 20: 1571–93.

Kumar, S.V., D.M. Mocko, S. Wang, C.D. Peters-Lidard, and J. Borak. 2019b. "Assimilation of Remotely Sensed Leaf Area Index into the Noah-MP Land Surface Model: Impacts on Water and Carbon Fluxes and States over the Continental United States." *Journal of Hydrometeorology* 20: 1359–77.

Kumar, S.V., C.D. Peters-Lidard, Y. Tian, P.R. Houser, J. Geiger, S. Olden, L. Lighty *et al*. 2006. "Land Information System: An Interoperable Framework for High Resolution Land Surface Modeling." *Environmental Modelling & Software* 21: 1402–15.

Kumar, S.V., C.D. Peters-Lidard, J. Santanello, K. Harrison, Y. Liu, and M. Shaw. 2012. "Land Surface Verification Toolkit (LVT) — A Generalized Framework for Land Surface Model Evaluation." *Geoscientific Model Development* 5: 869–86.

Kumar, S.V., C.D. Peters-Lidard, D. Mocko, and Y. Tian. 2013. "Multiscale Evaluation of the Improvements in Surface Snow Simulation through Terrain Adjustments to Radiation." *Journal of Hydrometeorology* 14: 220–32.

Kumar, S.V., R.H. Reichle, C.D. Peters-Lidard, R.D. Koster, X. Zhan, W.T. Crow, J.B. Eylander, and P.R. Houser. 2008. "A Land Surface Data Assimilation Framework Using the Land Information System: Description and Applications." *Advances in Water Resources* 31: 1419–32.

Kumar, S.V., S. Wang, D.M. Mocko, C.D. Peters-Lidard, and Y. Xia. 2017. "Similarity Assessment of Land Surface Model Outputs in the North American Land Data Assimilation System." *Water Resources Research* 53: 8941–65.

Kumar, S.V., B.F. Zaitchik, C.D. Peters-Lidard, M. Rodell, R. Reichle, B. Li, M. Jasinski *et al*. 2016. "Assimilation of Gridded GRACE Terrestrial Water Storage Estimates in the North American Land Data Assimilation System." *Journal of Hydrometeorology* 17: 1951–72.

Kundzewicz, Z.W., and P. Döll. 2009. "Will Groundwater Ease Freshwater Stress under Climate Change?" https://doi.org/10.1623/hysj.54.4.665.

Li, B., M. Rodell, S. Kumar, H.K. Beaudoing, A. Getirana, B.F. Zaitchik, L.G. de Goncalves *et al*. 2019. "Global GRACE Data Assimilation for Groundwater and Drought Monitoring: Advances and Challenges." *Water Resources Research* 55: 7564–86.

Li, B., M. Rodell, C. Peters-Lidard, J. Erlingis, S. Kumar, and D. Mocko. 2021. "Groundwater Recharge Estimated by Land Surface Models: An Evaluation in the Conterminous United States." *Journal of Hydrometeorology*. 22 (2): 499–522. http://dx.doi.org/10.1175/jhm-d-20-0130.1.

Liang, X., D.P. Lettenmaier, E.F. Wood, and S.J. Burges. 1994. "A Simple Hydrologically Based Model of Land Surface Water and Energy Fluxes for General Circulation Models." *Journal of Geophysical Research: Atmospheres* 99: 14415–28.

Liu, P.-W., R. Bindlish, B. Fang, V. Lakshmi, P. O'Neill, Z. Yang, M. Cosh *et al*. 2021. "Assessing Disaggregated SMAP Soil Moisture Products in the United States." *IEEE Journal of Selected Topics in Applied Earth Observations and Remote Sensing*. 1–5. http://dx.doi.org/10.1109/jstars.2021.3056001.

Liu, Z., P. Liu, E. Massoud, T.G. Farr, P. Lundgren, and J.S. Famiglietti 2019. "Monitoring Groundwater Change in California's Central Valley Using Sentinel-1 and GRACE Observations." *Geosciences* 9: 436.

Ma, N., G.-Y. Niu, Y. Xia, X. Cai, Y. Zhang, Y. Ma, and Y. Fang. 2017. "A Systematic Evaluation of Noah-MP in Simulating

Land-Atmosphere Energy, Water and Carbon Exchanges over the Continental United States." *Journal of Geophysical Research: Atmospheres* 122: 122–245.

McNally, A., K. Arsenault, S. Kumar, S. Shukla, P. Peterson, S. Wang, C. Funk, C.D. Peters-Lidard, and J.P. Verdin. 2017. "A Land Data Assimilation System for Sub-Saharan Africa Food and Water Security Applications." *Scientific Data* 4: 1–19.

Medellín-Azuara, J., D. MacEwan, R.E. Howitt, G. Koruakos, E.C. Dogrul, C.F. Brush, T.N. Kadir, T. Harter, F. Melton, and J.R. Lund. 2015. "Hydro-Economic Analysis of Groundwater Pumping for Irrigated Agriculture in California's Central Valley, USA." *Hydrogeology Journal* 23: 1205–16.

Meixner, T., A.H. Manning, D.A. Stonestrom, D.M. Allen, H. Ajami, K.W. Blasch, A.E. Brookfield *et al*. 2016. "Implications of Projected Climate Change for Groundwater Recharge in the Western United States." *Journal of Hydrology* 534: 124–38.

Mesinger, F., G. DiMego, E. Kalnay, K. Mitchell, P.C. Shafran, W. Ebisuzaki, D. Jović *et al*. 2006. "North American Regional Reanalysis." *Bulletin of the American Meteorological Society* 87: 343–60.

Miralles, D.G., T.R.H. Holmes, R.A.M. De Jeu, J.H. Gash, A.G.C.A. Meesters, and A.J. Dolman. 2011. "Global Land-Surface Evaporation Estimated from Satellite-Based Observations." *Hydrology and Earth System Sciences* 15: 453–69.

Mitchell, K.E., D. Lohmann, P.R. Houser, E.F. Wood, J.C. Schaake, A. Robock, B.A. Cosgrove *et al*. 2004. "The Multi-Institution North American Land Data Assimilation System (NLDAS): Utilizing Multiple GCIP Products and Partners in a Continental Distributed Hydrological Modeling System." *Journal of Geophysical Research: Atmospheres* 109. https://doi.org/10.1029/2003JD003823.

Mo, K.C., L.-C. Chen, S. Shukla, T.J. Bohn, and D.P. Lettenmaier. 2012. "Uncertainties in North American Land Data Assimilation Systems over the Contiguous United States." *Journal of Hydrometeorology* 13: 996–1009.

National Centers for Environmental Information. 2020. "Climate at a Glance." https://www.ncdc.noaa.gov/cag/statewide/rankings.

Niraula, R., T. Meixner, F. Dominguez, M. Rodell, H. Ajami, D. Gochis, and C. Castro. 2017. "How Might Recharge Change under Projected Climate Change in Western US?" *Geophysical Research Letters* 44: 10407–18.

Niu, G.-Y., and Z.-L. Yang. 2004. "Effects of Vegetation Canopy Processes on Snow Surface Energy and Mass Balances." *Journal of Geophysical Research: Atmospheres* 109. https://doi.org/10.1029/2004JD004884.

Niu, G.-Y., and Z.-L. Yang. 2006. "Effects of Frozen Soil on Snowmelt Runoff and Soil Water Storage at a Continental Scale." *Journal of Hydrometeorology* 7: 937–52.

Niu, G.-Y., Z.-L. Yang, R.E. Dickinson, L.E. Gulden, and H. Su. 2007. "Development of a Simple Groundwater Model for Use in Climate Models and Evaluation with Gravity Recovery and Climate Experiment Data." *Journal of Geophysical Research: Atmospheres* 112. https://doi.org/10.1029/2006JD007522.

Niu, G.Y., Z.L. Yang, K.E. Mitchell, F. Chen, M.B. Ek, M. Barlage, A. Kumar *et al*. 2011. "The Community Noah Land Surface Model with Multiparameterization Options (Noah-MP): 1. Model Description and Evaluation with Local-Scale Measurements." *Journal of Geophysical Research Atmospheres* 116: 1–19.

O'Neill, P.E., S. Chan, E.G. Njoku, T. Jackson, and R. Bindlish. 2016. *SMAP Enhanced L3 Radiometer Global Daily 9 Km EASE-Grid Soil Moisture, Version 1*. Boulder, CO: NASA National Snow and Ice Data Center Distributed Active Archive Center.

Ozdogan, M., M. Rodell, H.K. Beaudoing, and D.L. Toll. 2010. "Simulating the Effects of Irrigation over the United States in a Land Surface Model Based on Satellite-Derived Agricultural Data." *Journal of Hydrometeorology* 11: 171–84.

Peters-Lidard, C.D., P.R. Houser, Y. Tian, S.V. Kumar, J. Geiger, S. Olden, L. Lighty *et al*. 2007. "High-Performance Earth System Modeling with NASA/GSFC's Land Information System." *Innovations in Systems and Software Engineering* 3: 157–65.

Pinker, R.T., J.D. Tarpley, I. Laszlo, K.E. Mitchell, P.R. Houser, E.F. Wood, J.C. Schaake *et al*. 2003. "Surface Radiation Budgets in Support of the GEWEX Continental-Scale International Project (GCIP) and the GEWEX Americas Prediction Project (GAPP), Including the North American Land Data Assimilation System (NLDAS) Project." *Journal of Geophysical Research: Atmospheres* 108. https://doi.org/10.1029/2002JD003301.

Reichle, R.H., J.P. Walker, R.D. Koster, and P.R. Houser. 2002. "Extended versus Ensemble Kalman Filtering for Land Data Assimilation." *Journal of Hydrometeorology* 3: 728–40.

Rodell, M., P.R. Houser, U. Jambor, J. Gottschalck, K. Mitchell, C.-J. Meng, K. Arsenault *et al*. 2004. "The Global Land Data Assimilation System." *Bulletin of the American Meteorological Society* 85: 381–94.

Rodell, M., P.R. Houser, A.A. Berg, and J.S. Famiglietti. 2005. "Evaluation of 10 Methods for Initializing a Land Surface Model." *Journal of Hydrometeorology* 6: 146–55.

Scanlon, B.R., C.C. Faunt, L. Longuevergne, R.C. Reedy, W.M. Alley, V.L. McGuire, and P.B. McMahon. 2012. "Groundwater Depletion and Sustainability of Irrigation in the US High Plains and Central Valley." *Proceedings of the National Academy of Sciences of the United States of America* 109: 9320–5

Svoboda, M., D. LeComte, M. Hayes, R. Heim, K. Gleason, J. Angel, B. Rippey *et al*. 2002. "The Drought Monitor." *Bulletin of the American Meteorological Society* 83: 1181–90.

Swain, D.L. 2015. "A Tale of Two California Droughts: Lessons amidst Record Warmth and Dryness in a Region of Complex Physical and Human Geography." *Geophysical Research Letters* 42 (3): 9910–99.

Tang, Q., S. Peterson, R.H. Cuenca, Y. Hagimoto, and D.P. Lettenmaier. 2009. "Satellite-Based near-Real-Time Estimation of Irrigated Crop Water Consumption." *Journal of Geophysical Research: Atmospheres* 114. https://doi.org/10.1029/2008JD010854.

Tapley, B.D., S. Bettadpur, M. Watkins, and C. Reigber. 2004. "The Gravity Recovery and Climate Experiment: Mission Overview and Early Results." *Geophysical Research Letters* 31. https://doi.org/10.1029/2004GL019920.

Taylor, R.G., B. Scanlon, P. Döll, M. Rodell, R. van Beek, Y. Wada, L. Longuevergne *et al*. 2013. "Ground Water and Climate Change." *Nature Climate Change* 3: 322–9.

Verseghy, D.L. 1991. "Class — A Canadian Land Surface Scheme for GCMS. I. Soil Model." *International Journal of Climatology* 11: 111–33.

Wada, Y., L.P.H. van Beek, C.M. van Kempen, J.W.T.M. Reckman, S. Vasak, and M.F.P. Bierkens 2010. "Global Depletion of Groundwater Resources." *Geophysical Research Letters* 37. https://doi.org/10.1029/2010GL044571.

Wang, A., T.J. Bohn, S.P. Mahanama, R.D. Koster, and D.P. Lettenmaier. 2009. "Multimodel Ensemble Reconstruction of Drought over the Continental United States." *Journal of Climate* 22: 2694–712.

Wood, E.F., J.K. Roundy, T.J. Troy, L.P.H. van Beek, M.F.P. Bierkens, E. Blyth, A. de Roo *et al*. 2011. "Hyperresolution Global Land Surface Modeling: Meeting a Grand Challenge for Monitoring Earth's Terrestrial Water." *Water Resources Research* 47. https://doi.org/10.1029/2010WR010090.

Xia, Y., M. Ek, J. Sheffield, B. Livneh, M. Huang, H. Wei, S. Feng, L. Luo, J. Meng, and E. Wood. 2012. "Validation of Noah-Simulated Soil Temperature in the North American Land Data Assimilation System Phase 2." *Journal of Applied Meteorology and Climatology* 52: 455–71.

Xia, Y., D. Mocko, M. Huang, B. Li, M. Rodell, K.E. Mitchell, X. Cai, and M.B. Ek. 2017. "Comparison and Assessment of Three

Advanced Land Surface Models in Simulating Terrestrial Water Storage Components over the United States." *Journal of Hydrometeorology* 18: 625–49.

Xiao, Z., S. Liang, T. Wang, and B. Jiang. 2016. "Retrieval of Leaf Area Index (LAI) and Fraction of Absorbed Photosyn thetically Active Radiation (FAPAR) from VIIRS Time-Series Data." *Remote Sensing* 8. https://doi.org/10.3390/rs8040351.

Yang, Z.L., G.Y. Niu, K.E. Mitchell, F. Chen, M.B. Ek, M. Barlage, L. Longuevergne *et al*. 2011. "The Community Noah Land Surface Model with Multiparameterization Options (Noah-MP): 2. Evaluation over Global River Basins." *Journal of Geophysical Research Atmospheres* 116: 1–16.

Zeng, X., P. Broxton, and N. Dawson. 2018. "Snowpack Change from 1982 to 2016 over Conterminous United States." *Geophysical Research Letters* 45: 12–940.